

# MEASUREMENT OF THE INDUCED $\Lambda^0(1116)$ POLARIZATION IN $K^+$ ELECTROPRODUCTION at CLAS

M. Gabrielyan\*, B. Raue\*, D. S. Carman<sup>†</sup>, K. Park<sup>†</sup> and the CLAS  
Collaboration

\*Florida International University, Miami, FL 32306

<sup>†</sup>Thomas Jefferson National Accelerator Facility, Newport News, VA 23606

**Abstract.** We are using the  $p(e, e'K^+p)\pi^-$  reaction to perform a measurement of the induced polarization of the electroproduced  $\Lambda(1116)$  using its  $p\pi^-$  parity-violating weak decay. This study uses the CEBAF Large Acceptance Spectrometer (CLAS) to detect the scattered electron, the kaon, and the decay proton over the kinematics  $0.8 \leq Q^2 \leq 3.5 \text{ GeV}^2$ ,  $1.6 \leq W \leq 3.0 \text{ GeV}$ , and the full kaon CM angle range. In this experiment a 5.5 GeV electron beam was incident upon an unpolarized liquid-hydrogen target. The goal is to map out the kinematic dependencies for this polarization observable to provide new constraints for models of the electromagnetic production of  $K$ -hyperon final states. Along with previously published photo- and electroproduction cross sections and polarization observables from CLAS, SAPHIR, LEPS, and GRAAL, these data are needed in a coupled-channel analysis to identify previously unobserved  $s$ -channel resonances. Preliminary polarization results will be presented.

**Keywords:** kaon, hyperon, electroproduction, polarization.

**PACS:** PACS: 13.40.-f, 13.60Rj, 13.88.+e, 14.20.Gk, 14.20Jn

## INTRODUCTION

The strange quark plays an important role in understanding nucleon strong interactions. The present study is part of a larger program to measure as many observables as possible in kaon photo- and electroproduction, with the final goal of developing a comprehensive model of the strangeness production process. In this work, we have measured the induced polarization of the  $\Lambda(1116)$  from  $e + p \rightarrow e' + K^+ + \Lambda$ . The  $\Lambda$  decays via the weak interaction into either  $p\pi^-$  (64%) or  $n\pi^0$  (36%). Since parity is not conserved in the weak decay, the recoil  $\Lambda$  polarization can be extracted by measuring the angular distribution of the decay proton in the  $\Lambda$  rest frame. We will map out the dependence of the induced polarization as a function of the invariant energy  $W$ , the four-momentum transfer  $Q^2$ , and the center-of-momentum kaon scattering angle  $\theta_K^{CM}$ .

Within the framework of available theoretical approaches, these data, when combined with other electro- and photoproduction data, can help to identify the established nucleon resonances that couple to the  $KY$  final state and have the potential to help reveal the presence of previously unseen nucleon resonances that have been predicted by quark models [1]. Within the framework of recent coupled-channel approaches (see e.g. Refs. [2, 3, 4]), these new data should provide for valuable new constraints for future theoretical work.

## DATA ANALYSIS

The data for this experiment were taken using the Hall B CLAS spectrometer [5] at Jefferson Laboratory. A 5.5-GeV polarized electron beam was incident upon an unpolarized liquid-hydrogen target. The scattered electrons and the reaction products were detected in CLAS. These data span a  $Q^2$  range from 0.8 to 3.5  $\text{GeV}^2$ ,  $W$  from 1.6 to 3.0 GeV, and cover the full range of  $\theta_K^{CM}$ . This dataset contains more than 5 billion triggers. Approximately 213,000  $\Lambda$ s were analyzed.

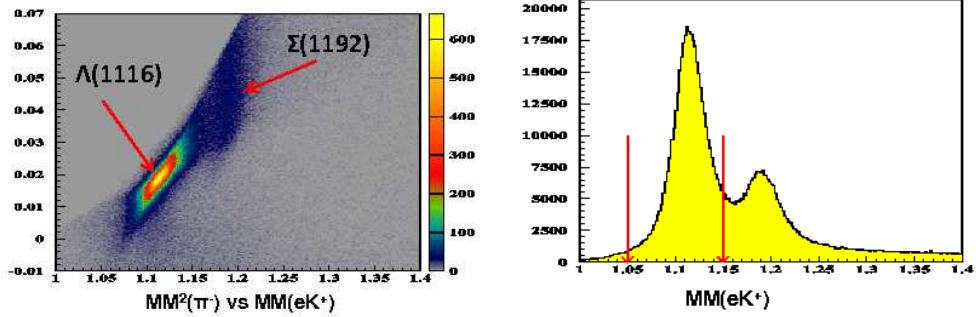


**FIGURE 1.** Correlation of  $MM^2(\pi^-)$  and  $MM(eK^+ p)$  (left) and the hyperon missing mass distribution (right). The arrows show the  $\Lambda$  mass cut applied for the analysis.

The data acquisition system was triggered by an electron candidate coincident in a Cherenkov counter and electromagnetic calorimeter segment. Hadrons are identified by calculating the time difference ( $\Delta t$ ) between the measured and computed times for a given hadron species ( $\pi^+, K^+, p$ ) using the minimum  $\Delta t$ . Hyperons are identified from the  $e'K^+$  final state missing mass. In order to reduce the background, a cut is applied on the  $eK^+ p$  missing mass, requiring it to be around the pion mass. Fig. 1 (left) shows the correlation between  $MM^2(eK^+ p)$  and  $MM(eK^+)$ . Fig. 1 (right) shows the  $MM(eK^+)$  spectrum with the requirement of a detected proton and the pion missing-mass cut.

The main source of background in the  $\Lambda$  missing-mass spectrum is from pions misidentified as kaons. Due to the CLAS resolution, the  $\Lambda$  and  $\Sigma^0$  peaks are not fully separated. The  $\Sigma^0$  contribution beneath the  $\Lambda$  peak is accounted for by fitting during background subtraction. In order to achieve reliable fits, the  $MM^2(eK^+ p)$  cut is extended to include all  $\Sigma^0$ 's. The fit function form was chosen based on  $\Lambda$  and  $\Sigma^0$  Monte Carlo templates. Typical fit examples are shown in Fig. 2 for  $0.8 < \cos \theta_K^{CM} < 1.0$  and different  $W$  bins. The  $\Lambda$  missing-mass distributions for forward and backward moving  $p$ 's, with respect to coordinate axes associated with the  $\Lambda$  rest frame, are fit simultaneously. The background subtracted, uncorrected  $\Lambda$  yields are extracted in the mass range from 1.05 to 1.15 GeV.

The angular distribution of the decay protons in the  $\Lambda$  rest frame is given by:

$$\frac{dN}{d\cos(\theta_p^{RF})} = N_0 \cdot (1 + \alpha P_\Lambda \cos \theta_p^{RF}),$$

where  $N_0$  is a normalization factor,  $\alpha$  is the  $\Lambda$  weak decay asymmetry parameter ( $\alpha = 0.642 \pm 0.013$  [6]),  $P_\Lambda$  is the average induced polarization, and  $\theta_p^{RF}$  is the proton angle in the  $\Lambda$  rest frame with respect to a given spin-quantization axis. The polarization results

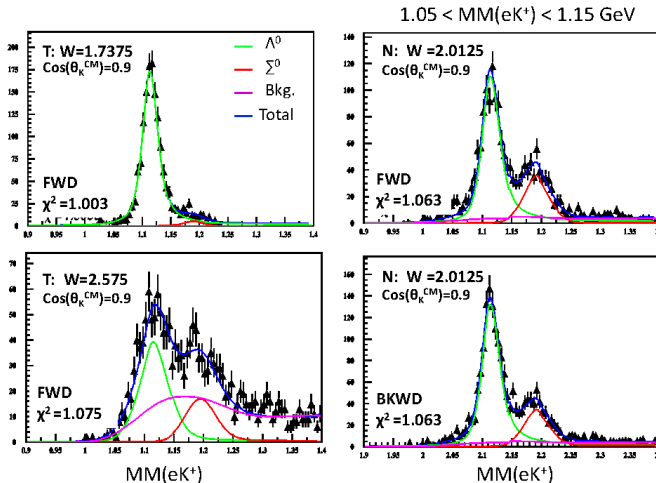


**FIGURE 2.** Typical fits to missing mass histograms at  $0.8 < \cos \theta_K^{CM} < 1$  for different  $W$  bins. FWD and BKWD in these plots refer to  $\cos \theta_p^{RF} > 0$  and  $\cos \theta_p^{RF} < 0$ , respectively.  $T$  refers to the axis orthogonal to the  $\Lambda$  momentum vector in the hadronic plane and  $N$  refers to the axis normal to the hadronic reaction plane.

are calculated via the forward-backward asymmetry (relative to  $\cos \theta_p^{RF}=0$ ) as:

$$P_\Lambda = \frac{2}{\alpha} \cdot \frac{N_F - N_B}{N_F + N_B}.$$

$N_F$  and  $N_B$  are defined for each spin-quantization axis as the yield of protons moving along ( $N_F$ ) or opposite ( $N_B$ ) to the axis. Here  $N_F$  and  $N_B$  are the background-subtracted, acceptance-corrected yields. The acceptance corrections are determined with a full-scale GEANT simulation of the reaction, using a phase space generator with a modified  $t$ -slope. In order to increase the statistics in each kinematic bin, the results are summed over  $\Phi$ , the relative angle between the electron and hadron planes. For the induced polarization, the relevant spin-quantization axis is normal to the  $K^+ \Lambda$  reaction plane. With the  $\Phi$  integration, the longitudinal (along the  $\Lambda$  direction) and transverse components of the polarization vanish [7]. This provides a valuable check on our systematics. The analysis shows that unlike the longitudinal and the transverse components of the induced polarization, the normal component is practically insensitive to acceptance corrections. The upper limit on systematic uncertainties is estimated to be  $< 0.1$ . Preliminary polarization results vs.  $W$  are shown in Fig. 3 for two  $\cos \theta_K^{CM}$  bins. During the course of the analysis we found that the polarization was independent of  $Q^2$ , which allowed us to integrate over this variable.

The polarization shows a strong dependence on  $W$  up to about 2.0 GeV at all but the most forward-angle bin ( $0.8 < \cos \theta_K^{CM} < 1$ ). This suggests sensitivity to  $s$ -channel processes. In the forward-angle bin, where  $t$ -channel processes dominate, the data are rather flat with  $W$ . A similar strong  $W$  dependence of the polarizations is observed at mid-range angles in the CLAS photoproduction data [8]. The sharp change of sign in the polarization is not observed in electroproduction data. At forward angles the CLAS photoproduction polarization is again flat.

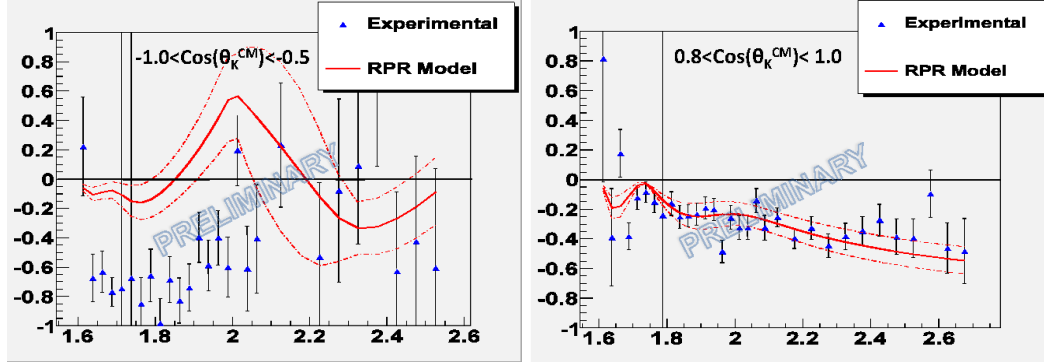


**FIGURE 3.** Preliminary  $\Lambda$  induced polarization vs.  $W$  for two  $\cos \theta_K^{CM}$  bins. The results are integrated over  $Q^2$  and  $\Phi$ . The curves are the RPR model predictions with their uncertainties [9].

Results are compared with the Ghent RPR model predictions [9]. Non-resonant background contributions in this model are treated as exchanges of kaonic Regge trajectories. To take into account the  $s$ -channel contributions at mid-angles, RPR includes the established resonances  $S_{11}(1650)$ ,  $P_{11}(1710)$ ,  $P_{13}(1720)$ ,  $P_{13}(1900)$ , and the missing resonance  $D_{13}(1900)$ . It was fit to forward angle ( $\cos \theta_K^{CM} > 0$ ) photoproduction data (CLAS, LEPS, GRAAL) to constrain the parameters. RPR calculations are in good agreement with experimental data at very forward kaon angles but they fail to reproduce the data at all other kaon angle bins (Fig. 3 solid curves).

## CONCLUSION

This work is part of a larger program to measure cross sections and polarization observables in kaon photo- and electroproduction, with our main goals to better understand which  $s$ -channel resonances couple to strangeness and to improve theoretical descriptions of the associated reaction mechanism. We expect that when the analysis is finalized, these new polarization data, covering a broad kinematic range, will help to improve the constraints to ongoing coupled-channel analyses.

This work is funded in part by the U.S. Dept. of Energy and the Graduate School at Florida International University.

## REFERENCES

1. S. Capstick and W. Roberts, Phys. Rev. D **58**, 74011 (1998).
2. B. Julia-Diaz et al., Phys. Rev. C **73**, 055204 (2006).
3. A. V. Sarantsev et al., Eur. Phys. J. A **25**, 441 (2005).
4. A. V. Anisovich et al., Eur. Phys. J. A **34**, 243 (2007).
5. B. A. Mecking et al., Nucl. Inst. and Meth. A**503**, 513 (2003).
6. S. Eidelman et al. (PDG), Review of Particle Physics, Phys. Lett. B **592**, 1 (2004).
7. D. S. Carman et al. (CLAS Collaboration), Phys. Rev. Lett. **90**, 131804 (2003); Phys. Rev. C**79**, 065205 (2009).
8. M. E. McCracken et al. (CLAS Collaboration), Phys. Rev. C**81**, 025201 (2010).
9. T. Corithals et al., Phys. Lett. B **656**, 186 (2007).